The Linear Viscoelastic Properties of Copolypropylene–Clay Nanocomposites

Weixia Zhong,[1] Xiuying Qiao,[1] Kang Sun,[1] Guoding Zhang,[1] Xiaodong Chen[2]

[1]*State Key Laboratory of Metal Matrix Composites, Shanghai Jiao Tong University, Shanghai 200030, People's Republic of China*
[2]*Shanghai Sunny New Technology Development Co., Ltd., Shanghai 201108, China*

Received 3 April 2005; accepted 14 May 2005
DOI 10.1002/app.22244
Published online in Wiley InterScience (www.interscience.wiley.com).

ABSTRACT: The linear viscoelastic properties of copolypropylene (cPP)–clay nanocomposites (cPPCNs) prepared by melt intercalating with different amounts of clay were extensively examined by rheological measurements. Meanwhile, the clay effects on the cPP confinements were first estimated by calculating the activation energy of different cPP moving units, including the whole molecular chain, the chain segment, and smaller unit such as chain link. The results showed that the stability of cPPCNs melts wrecked when the clay loading was above 5 wt %. An increase in clay loading of cPPCNs gave rise to a strong low frequency solid-like response ($G' > G''$). Unlike the matrix polymer, cPPCN5 (with 5 wt % clay) exhibited a relaxation plateau as relaxation time prolonged above 100 s, and displayed a maximal linear modulus. The variations of the activation energy of different cPP moving units revealed that the mobility of cPP molecular chains was restricted by clay layers, while these restrictions were not only related to the clay loadings but also largely depended on the clay dispersion status in the matrix. The motions of cPP chain segments were greatly limited at 3–5 wt % loading of clay, but drastically activated with the addition of 7 wt % clay due to the increasing stacks of clay layers within the matrix. However, it was found that the presence of clay had little effect on the mobility of small cPP moving units such as chain links. © 2005 Wiley Periodicals, Inc. J Appl Polym Sci 99: 1523–1529, 2006

Key words: copolypropylene; rheology; composites; clay; viscoelastic properties; the activation energy

INTRODUCTION

Recently, blending of many types of clay into thermoplastic matrices to form new materials has been an effective way and attracted considerable technological and scientific interests due to the dramatic enhancements in physical, thermal, and mechanical properties. Previous reports of polymer–clay nanocomposites are plenteous. Nevertheless, they are mainly focused on the preparation, structures, and thermal/mechanical properties.[1–11] Rheological studies on polymer–clay nanocomposites are relatively few, especially on the cPP matrix nanocomposites. However, the rheological properties are not only indicative of melt-processing behavior but also sensitive to the structure, particle size, shape, and surface characteristics of the dispersed phase in composites. Moreover, rheology potentially offers a means to assess the state of dispersion of nano-fillers in the melt state. Therefore, it would be of great significance to relate the melt properties to the microstructure of the polymer–clay nanocomposites via rheological observations.

Correspondence to: K. Sun (ksun@sjtu.edu.cn).

Journal of Applied Polymer Science, Vol. 99, 1523–1529 (2006)

Unlike the matrices, the polymer–clay nanocomposites exhibited some particular rheological properties. For example, the melts of intercalated poly(dimethyl-*co*-diphenylsiloxane) based nanocomposites[12] possessed unusual viscoelastic properties such as the nonterminal dynamic moduli at low frequency and a high shear thinning tendency. For end-tethered poly(ε-caprolactone) and nylon 6 exfoliated nanocomposites,[13] significant differences in the rheological properties were also observed. The low-frequency storage and loss moduli gradually changed from liquid-like to a pseudosolid-like behavior when merely 3 wt % clay was added. As for model monodisperse polystyrene–polyisoprene diblock copolymers,[1] the rheology of the melts was not affected by the chemical nature of the polymer matrix but rather by the mesoscopic structure of the composites. In contrast, for polypropylene (PP) nanocomposites,[14–16] research work indicated that such materials showed a Newtonian response with a high viscosity at low strain rate, an apparent yield-like behavior, as well as an enhanced tensile modulus, much enhanced melt tension, and reduced neck-in during melt processing as compared with neat polymer. Moreover, PP nanocomposites exhibited microstructural changes during annealing period. Nevertheless, the viscoelastic characterizations performed by polymer–clay systems are highly different, with

TABLE I
Results of the Stability of All Samples

Sample	Compositions	$\eta^*(t_0)$ (Pa s)	$\eta^*(t_{2000s})$ (Pa s)	Stable time (s)
cPPCN0	cPP/MAH-*g*-iPP (79/21)	13.0	13.0	0
cPPCN3	cPP/MAH-*g*-iPP/$OMMT_1$ (76/21/3)	60.6	62.2	50
cPPCN5	cPP/MAH-*g*-iPP/$OMMT_1$ (74/21/5)	80.0	83.6	500
cPPCN7	cPP/MAH-*g*-iPP/$OMMT_1$ (72/21/7)	16.0	33.1	>2000

dramatic alterations to the structure of polymer–clay composites.[17,18]

In this article, the linear viscoelastic properties of copolypropylene (cPP)–clay nanocomposites (cPPCNs) prepared by melt intercalation with different amounts of orgnophilic clay were extensively studied. Meanwhile, it is notable that the effects of clay loadings on the cPP confinements were firstly estimated by calculating the activation energy of different cPP moving units, including the whole molecular chain, the chain segment, and smaller unit such as chain link.

EXPERIMENTAL

Materials

The cPP matrix for the composites was copolypropylene SB9430 (MFI = 30 g/10 min, ρ = 0.91 g/cm^3) produced by Korea PetroChemical IND. CO., LTD. The compatibilizer used was maleic anhydride grafted polypropylene (MAH-*g*-PP) provided by Shanghai Sunny New Technology Development Co., LTD, having 1.0% MAH content. The clay, octadecylammonium-modified montmorillonite (C_{18}–MMT), was supplied by Fenghong clay Co., China.

Sample preparation

A series of cPP–clay nanocomposites (cPPCNs) were prepared by melt intercalation in a thermoplastic mixer of Rheocord 900 Haake. Among cPPCNs, the loading of clay was changed from 0 to 7 wt %, and the compositions of the resulting composites were given in Table I. Melt intercalation was performed at 180°C with a rotor speed of 100 rpm for 10 min, and the obtained composites were compression-molded into pieces of 100 × 100 × 1 mm^3 disks. Molding was carried out at 180°C followed by slow cooling under pressure.

X-ray diffraction (xrd)

The interlayer spacing of clay in composites was studied at ambient temperature by using an X-ray Diffractometer (D/MAXIII, Japan), with a Cu Kα radiation (λ = 0.154 nm). All the samples were scanned by plates over a 2θ range of 1°–11° at a rate of 2°/min. As for these samples, the interlayer spacing of clay was determined from the[1] reflection peak in the XRD patterns.

Rheological measurements

The melt-state viscoelastic properties for the intercalated copoly(propylene)–clay nanocomposites (cPPCNs) were investigated using a strain controlled rheometer (ARES Rheometer, Rheometrics Scientific, USA), with a parallel plate geometry using 25 mm diameter plates. All rheological measurements were done under ambient atmosphere at 180°C and the gap was set at 0.8–1 mm. In these measurements, dynamic time sweeps were carried out to investigate the thermal stability of samples as a function of time at 6.28 rad/s and a linear strain of 0.5%. Dynamic strain sweeps were done to determine the linear regime of samples. And then, the linear viscoelastic properties were observed by frequency-sweep experiments, stress relaxation measurements, and creep tests. Additionally, the activation energy of cPP molecular chains could be measured from creep data.

Dynamic mechanical analysis (DMA)

Dynamic mechanical analysis was carried out on Rheometrics Dynamic Mechanical Analyzer (DMA IV). Test samples were bars (about 15 mm length, 4 mm width) cut from the compression-molded plaques. The experiments were performed in a single-point bending mode over a wide frequency range (0.1, 1, 5, and 10 Hz) with a temperature range from –100 to 150°C and a heating rate of 3°C/min under a controlled sinusoidal strain. The loss factor ($\tan\delta = E'/E''$) was recorded as a function of temperature and frequency. Consequently, the activation energy of cPP chain segments and smaller moving units such as cPP chain links were also calculated from the DMA data.

RESULTS AND DISCUSSION

Microstructure

X-ray diffraction patterns for the pure clay and its composites with different clay loadings are presented in Figure 1. As shown in Figure 1, the virgin clay exhibits a single diffraction peak at about 4.1°, corresponding to an interlayer spacing of 2.1 nm. After

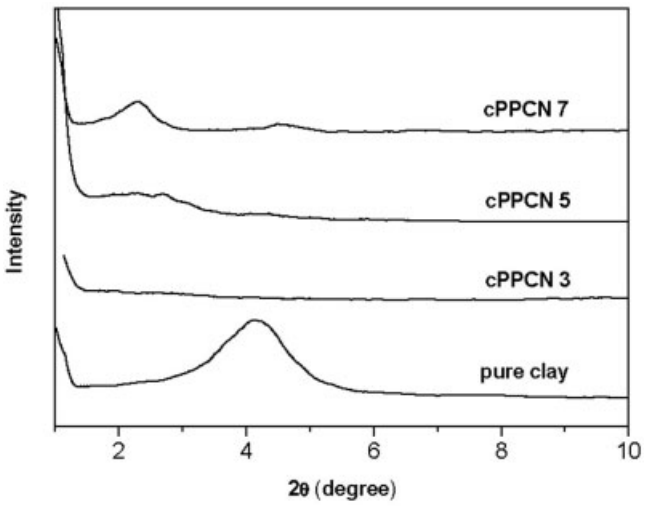

Figure 1 X-ray diffraction patterns of clay and its composites (cPPCN3, cPPCN5, and cPPCN7).

compounding clay into the polymer matrix, the clay displays different diffraction peaks. With 3 wt % loading of clay, the diffraction pattern is featureless, indicating a complete exfoliation of clay platelets in cPPCN3. The pattern of cPPCN5 shows a weak and broad peak. In contrast, the pattern of cPPCN7 appears a clear diffraction peak at 2.4°, which implies that more stacks of clay layers exist in cPPCN7. Thus, it can be concluded that the loading of clay directly affects the exfoliation status of clay layers within the polymer matrix.

Linear viscoelastic characterization

Melt stability

To investigate the melt stability during the period of measurements, dynamic time sweeps on polymer matrix (cPPCN0), and cPP–clay nanocompsoites (cPPCN3, cPPCN5, and cPPCN7) were measured at a linear strain of 0.5%, the spectra of dynamic viscosity (η^*) vs. time (t) are shown in Figure 2, and the detail information is also given in Table I. As seen from Figure 2, the cPPCN0 is stable in the examined time, since the η^* is invariable during 2000 s sweep. For cPP–clay composites, the melt stability displays some difference due to different contents of clay. The η^* of cPPCN3 is independent of time within 2000 s, the same as cPPCN0. The η^* of cPPCN5 increases from 80.0 to 83.6 Pa s for the first 500 s and then leveled off for the next 1500 s, indicating a slight structure perfection of cPPCN5 during a short time. Contrastingly, the η^* of cPPCN7 rapidly increases at the initial time of 800 s followed by a slow increase at the latter 1200 s, which suggests that the melt structure of cPPCN7 is not stable and would be changed as the annealing time prolonged. Therefore, the melt stability of the resulting cPP–clay composites is sensitive to the clay loadings. Associated with the previous analysis of XRD patterns, the cPPCN melts is found to be relative to the clay dispersion status within the matrix. A nearly complete exfoliation structure of cPP–clay composite has a stable melt structure, and such stability decreases with stacks of clay layers increasing.

Thus, in the following rheological tests, all the samples were annealed for 1000 s before starting measurements to ensure the sample to be in their equilibrium states.

Linear regimes

Figure 3 shows the storage modulus (G') obtained from dynamic strain sweeps for the matrix polymer and its composites. The transition from the linear to the nonlinear regime (namely, the critical strain), characterized by a rapid decrease in G', occurs at about 12% strain for the matrix polymer. For cPP–clay composites, such transition shifts toward a smaller strain as clay loading increases, at about 10% strain for cPPCN3, 4% strain for cPPCN5, and 3% strain for cPPCN7. Complementally, the linear G' of cPPCN5 is higher than that of the polymer matrix and two other cPP–clay composites (cPPCN3 and cPPCN7), in agreement with the variations of η^* in dynamic time sweeps.

Dynamic viscoelasticity

To ensure the rheological characterizations in the linear regime, as well as in the same testing state, small amplitude dynamic frequency-sweep experiments were performed at 12, 10, 4, and 3% strain for cPPCN0,

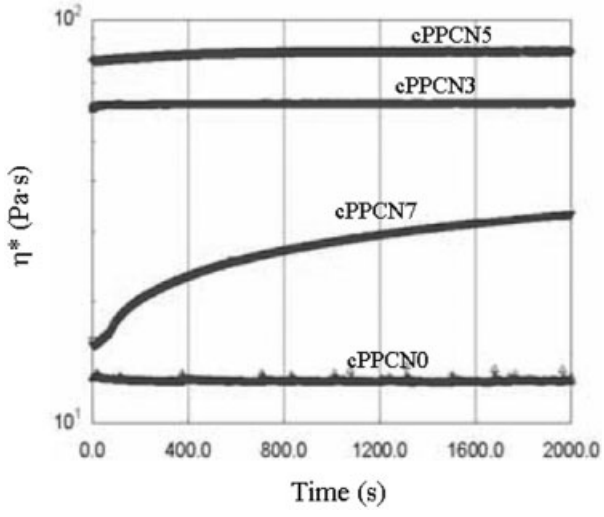

Figure 2 Dynamic time sweeps for PPCN0, cPPCN3, cPPCN5, and cPPCN7 at 180°C, 6.28 rad/s, and a linear strain of 0.5%.

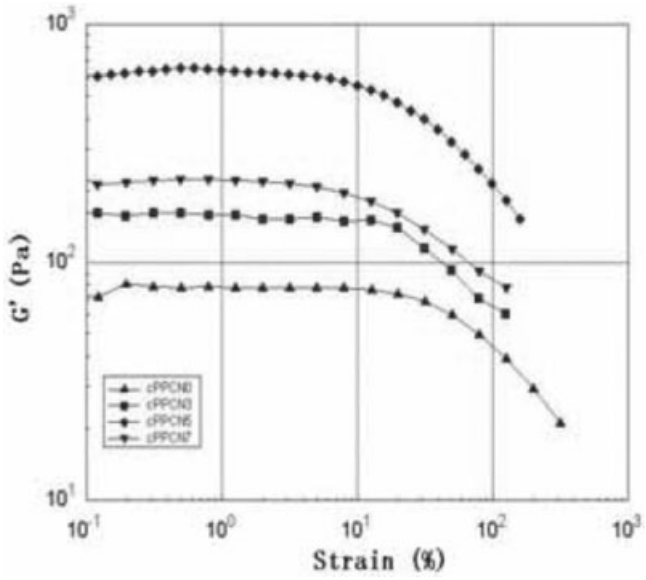

Figure 3 Dynamic storage modulus (G') of different cPP nanocomposites in strain sweeps at 180°C and 6.28 rad/s.

cPPCN3, cPPCN5, and cPPCN7, respectively, and the linear dynamic viscoelastic curves are shown in Figure 4. The matrix polymer (cPPCN0) shows apparent liquid-like behavior ($G' < G''$) at low frequency. In contrast, cPPCNs exhibit a solid-like response ($G' > G''$) at low frequency with clay loadings increasing in that a crossover ($G' = G''$) of cPPCN3, cPPCN5, and cPPCN7 occurs at 0.019 rad/s, 0.032 rad/s, and 0.20 rad/s, respectively. The higher frequency crossover with greater clay loadings indicates the stronger solid-like response. To further probe the solid-like performance of those nanocomposites, terminal zone slopes (at low frequency) of samples were calculated on the double logarithmic plot and listed in Table II. At low frequencies, the power-law dependence of G' and G'' in different composites decreases as clay loading increases, and appears almost invariant with frequency decreasing, far deviating from the terminal behavior ($G'' \sim \omega$, $G' \sim \omega^2$ at low frequency). These phenomena confirm the solid-like response of cPPCN melts with clay loadings, which is similar to the earlier reports for other polymer–clay nanocomposites.[12–15]

Linear stress relaxation

To further observe the unusual viscoelastic behaviors of cPP–clay nanocomposites, the stress relaxation measurements were performed on all the samples after step strain. According to the strain sweep data (Fig. 3), the linear step strain of 12, 5, 2, and 1% were respectively, used for cPPCN0, cPPCN3, cPPCN5, and cPPCN7, and the resultant relaxation modulus ($G(t)$) as a function of time are shown in Figure 5. It is obvious that the $G(t)$ for cPP–clay composites is higher than that for the matrix polymer, and the increment exhibits some differences owing to different clay loadings. The matrix polymer (cPPCN0) relaxed like a liquid at times longer than 15 s, whereas the cPP–clay composites relaxed slowly after the initial rapid relaxation and reached a plateau at relatively long times of 100 s, behaving like a solid. Furthermore, the higher $G(t)$ of cPPCN5 than cPPCN7 implies that the 5 wt % clay is an optimum content for resisting the stress relaxation. This result is in conformity with the tendency of linear modulus, which correlates closely with the dispersion of clay layers. In cPP–clay composites, 7 wt % loading of clay led to a poor stack dispersion of clay layers, with respect to the loading of 5 wt %.

Calculation of the activation energy

To investigate the affinity between the matrix and clay, the effects of clay loadings on the cPP molecules confinement were estimated by calculating the activation energy of cPP chains, chain segments, and smaller moving units such as chain links. As referred to previous research work,[19–20] the dependence of viscosity upon temperature is governed by the Arrhenius equation:

$$\ln \eta_0 = \ln A + \frac{\Delta E_f}{RT} \tag{1}$$

where η_0 is the zero-shear viscosity, A, a constant, R, the gas constant, and ΔE_f, the activation energy for an elementary flow process. A plot of ln η_0 against $1/T$ gives a straight line of slope $\Delta E_f / R$. Therefore, if η_0 is known, the activation energy of cPP chains (ΔE_f) for different melts could be calculated.

It has been reported that η_0 could be obtained from the creep data.[14,20] Figure 6 shows the creep compliances ($J(t)$) for the matrix and cPP–clay composites as a function of time at 180°C and a linear stress of 7 Pa. As seen from Figure 6, the $J(t)$ of cPPCN samples was significantly lower than that of the matrix polymer, and decreased with clay loadings, also indicating the strong solid-like response of cPP–clay composites.

To obtain the temperature dependence of viscosity, creep experiments on all samples were performed by a linear stress at temperature of 180, 190, and 200°C, respectively. According to the eq. (1), the flow activation energy of cPP molecular chains (ΔE_f) for all samples were calculated (see Fig. 7) and listed in Table II. It is observed that the ΔE_f of cPP–clay composites increases and the ΔE_f of cPPCN5 is higher than those of cPPCN3 and cPPCN7. These results reflect that blending of clay into the matrix polymer causes some energetic barrier for the motions of cPP molecular chains. Moreover, such energetic barrier attains a max-

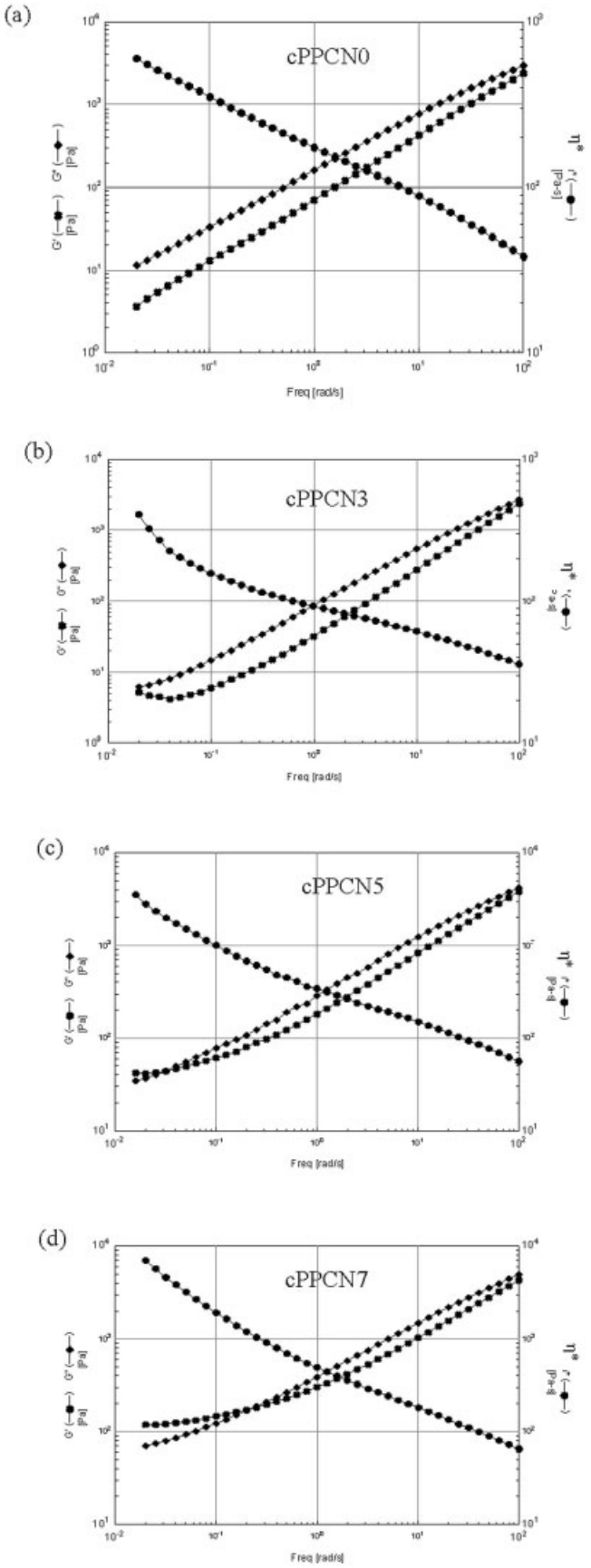

Figure 4 Small amplitude frequency sweep data at 180°C for cPPCNs. (a) cPPCN0 (strain = 12%), (b) cPPCN3 (strain = 10%), (c) cPPCN5 (strain = 4%), and (d) cPPCN7 (strain = 3%).

TABLE II
The Activation Energy and Terminal Slope (G' and G'' versus ω) of All Samples

Sample	Frequency sweep G′	Frequency sweep G″	ΔE_f (KJ/mol)	$\Delta E_{a\mathrm{I}}$ (KJ/mol)	$\Delta E_{a\mathrm{II}}$ (KJ/mol)
cPPCN0	0.723	0.677	12.11	361.2	263.4
cPPCN3	0.635	0.602	18.29	462.9	262.3
cPPCN5	0.398	0.476	25.94	432.1	287.5
cPPCN7	0.228	0.457	18.62	191.2	232.3

imal value when 5 wt % clay was added, which should be attributed to the dispersion of clay layers. In cPPCN7, owing to more stacks distribution of clay layers, the clay confinement on cPP molecular chains is weakened. Nevertheless, it is notable that these results are different from the work of Galgali[14] or Gu.[21] The differences should be correlated with the different microstructures.

On the other hand, it is possible to interrelate the temperature at which a relaxation process is observed (T) with the frequency of excitation (f) by the Arrhenius equation :[22]

$$\ln f = \ln f_0 + \frac{-\Delta E_a}{RT} \tag{2}$$

Here f_0 is a constant, f, the frequency of the test, R, the gas constant, and ΔE_a, the activation energy of the relaxation process. Similarly, the relaxation energy ΔE_a could be obtained by the slope of the straight line of $\ln f$ vs. $1/T$.

The effect of frequency on the cPP relaxation temperature could be analyzed by DMA; consequently, the activation energies of cPP chain segments and smaller units (such as chain links) could be measured.

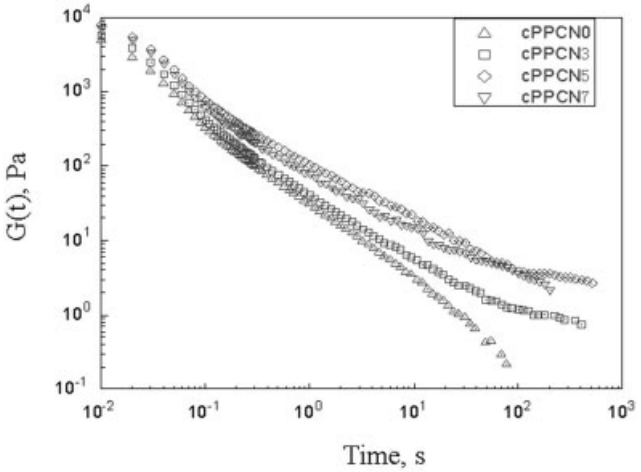

Figure 5 Stress relaxation data after step strain for cPPCN0, cPPCN3, cPPCN5, and cPPCN7.

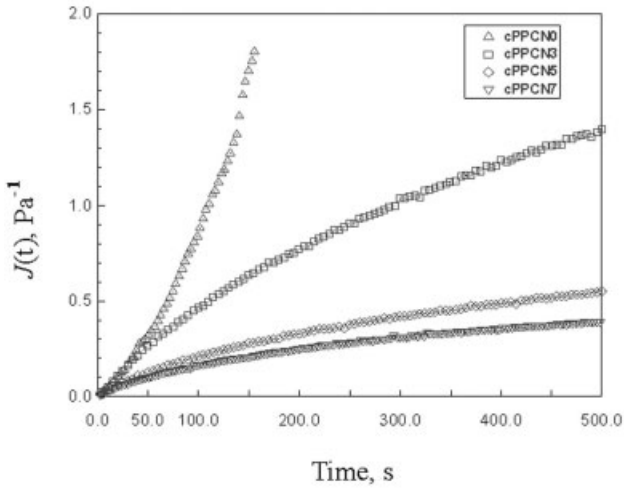

Figure 6 Creep compliances of cPPCN0, cPPCN3, cPPCN5, and cPPCN7 at 180°C for a stress of 7 Pa.

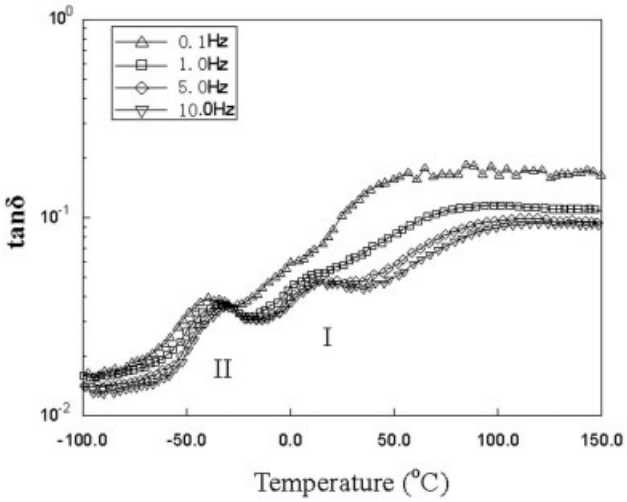

Figure 8 Effect of the frequency on DMA spectra of the matrix polymer (cPPCN0).

DMA tests were performed on all samples over a temperature range of –100 to 150°C and at four different frequencies (0.1, 1, 5, and 10 Hz). In Figure 8, the temperature dependence of tanδ for the matrix polymer (cPPCN0) is presented typically. The tanδ curve of the cPPCN0 exhibits two relaxation peaks, located at I and II positions (as seen from Fig. 8), which correspond to the relaxing unit of cPP chain segments in amorphous regions and the small relaxing unit such as the cPP chain links, respectively,.[23] It is obvious that the relaxing I-peak and II-peak both shift to higher temperature as the frequency increases. The activation energy of cPP chain segments ($\Delta E_{a\mathrm{II}}$) and the activation energy of smaller cPP moving unit such as chain links ($\Delta E_{a\mathrm{II}}$) for all samples are calculated by the above eq. (2) (see Fig. 9) and their results are listed in Table II. As seen from the $\Delta E_{a\mathrm{II}}$ values in Table II, the presence of clay platelets have little effect on the motions of small cPP relaxing units such as chain links. Contrastingly, the $\Delta E_{a\mathrm{I}}$ greatly increases in cPPCN3 and cPPCN5, but sharply decreases in cPPCN7. This result is also attributed to the dispersion of clay platelets, which could be accounted for that when the clay loadings was lower than 5 wt %, the clay platelets could be fully exfoliated and well dispersed within the matrix polymer, and consequently, strong barriers on the motions of cPP chain segments in amorphous regions.

Above all, addition of 5 wt % clay led to a strong effect on the motions of cPP molecules, reflecting a close affinity between cPP molecules and clay layers.

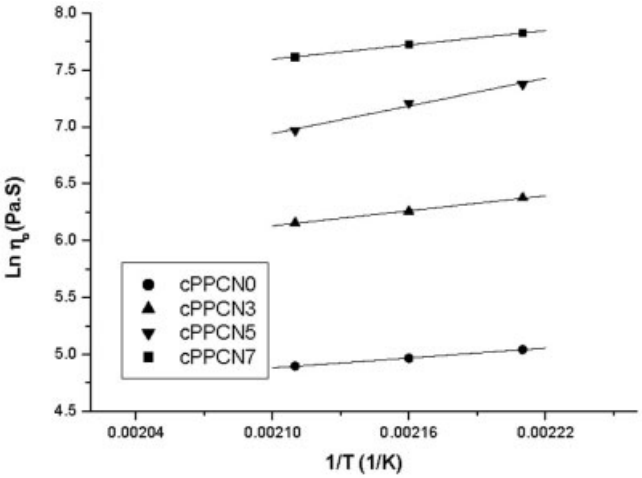

Figure 7 Arrhenius plot of zero-shear viscosity as a function of temperature.

CONCLUSIONS

The linear viscoelastic properties for copoly(propylene)–clay nanocomposites (cPPCNs) with clay loading from 0 to 7 wt % were examined by rheological measurements in this article. The dynamic time sweeps showed that the structure stability of cPPCNs melts wrecked when the clay loading was 7 wt %, which correlates with the existence of more stacks of clay layers in composites. The cPP–clay composites exhibited a solid-like response ($G' > G''$) at low frequency, and a low frequency crossover ($G' = G''$) was observed and shifted towards higher frequency with clay loadings. Unlike the matrix polymer (cPPCN0), the cPPCNs exhibited a relaxtion plateau as time prolonged above 100 s and an enhanced relaxtion modulus ($G(t)$). The linear modulus of cPP composites exhibited a maximum at 5 wt % clay loading, which could be attributed to the good dispersion of clay layers in cPPCN5. Furthermore, the cPP confinements caused by clay loadings were estimated by calculating the action energy of different cPP moving units. The flow

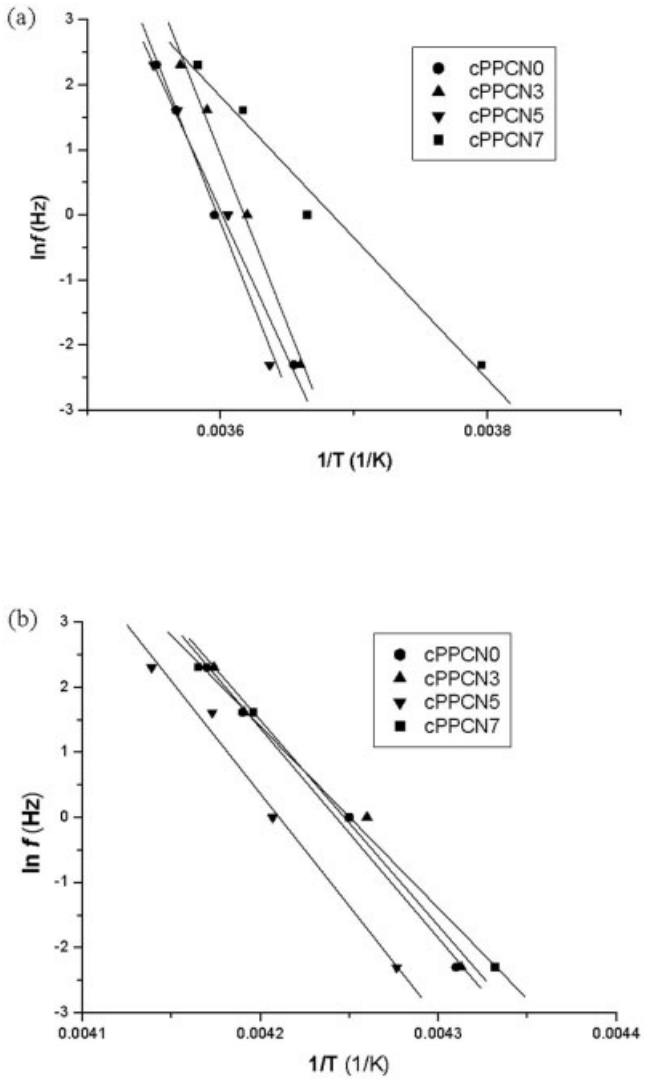

Figure 9 Calculation of the action energy of different cPP moving units. (a) cPP chain segments ($\Delta E_{a\mathrm{I}}$); (b) smaller cPP moving units such as chain links ($\Delta E_{a\mathrm{II}}$).

activation energy of cPP molecular chains (ΔE_f) increased due to the presence of clay, and attained a maximum at 5 wt % loading, which revealed that the motions of cPP molecular chains were restricted by clay platelets, while such restriction was related to not only the amounts of clay but also the exfoliated extent of the clay layers. The great increase of activation energy of cPP chain segments ($\Delta E_{a\mathrm{I}}$) in cPPCN3 and cPPCN5 followed by a sharp decrease in cPPCN7 indicated that the cPP chain segments motions were greatly limited at 3–5 wt % clay, but dramatically activated as the clay increased to 7 wt % (the $\Delta E_{a\mathrm{I}}$ of cPPCN7 is far lower than that of cPPCN0), due to the increasing stacks of clay layers. However, addition of clay had little effect on the activation energy of small cPP moving unit such as chain links ($\Delta E_{a\mathrm{II}}$), suggesting little influence on the mobility of small cPP relaxing units.

References

1. Ren, J. X.; Silva, A. S.; Krishnamoorti, R. Macromolecules 2000, 33, 3739.
2. Kim, K. N.; Kim, H.; Lee, J. W. Polym Eng Sci 2001, 41, 1963.
3. Hasegawa, N.; Okamoto, H.; Kato, M.; Usuki, A. J Appl Polym Sci 2000, 78, 1918.
4. Ma, J. S.; Qi, Z. N.; Hu, Y. L. J Appl Polym Sci 2001, 82, 3611.
5. Kawasumi, M.; Hasegawa, N.; Kato, M.; Usuki, A.; Okada, A. Macromolecules 1997, 30, 6333.
6. Maiti, P.; Nam, P. H.; Okamoto, M.; Hasegawa, N.; Usuki, A. Macromolecules 2002, 35, 2042.
7. Fu, X.; Qutubuddin, S. Polymer 2001, 42, 807.
8. Chiu, F. C.; Lai, S. M.; Chen, J. W.; Chiu, P. H. J Polym Sci Part B: Polym Phys 2004, 42, 4139.
9. Feng, M.; Gong, F. L.; Zhao, C. G.; Chen, G. G.; Zhang, S. M.; Yang, M. S.; Han, C. C. J Polym Sci Part B: Polym Phys 2004, 42, 3428.
10. Xu, W. B.; Ge, M. L.; He, P. S. J Polym Sci Part B: Polym Phys 2002, 40, 408.
11. Zheng, W. G.; Lu, X. H.; Toh, C. L.; Zheng, T. H.; He, C. B. J Polym Sci Part B: Polym Phys 2004, 42, 1810.
12. Krishnamoorti, R.; Vaia, R. A.; Giannelis, E. P. Chem Mater 1996, 8, 1728.
13. Kishnamoorti, R.; Ginannelis, E. P. Macromolecules 1997, 30, 4097.
14. Galgai, G.; Ramesh, C.; Lele, A. Macromolecules 2001, 34, 852.
15. Solomon, M. J.; Almusallam, A. S.; Seefeldt, K. F.; Somwangthanaroj, A.; Varadan, P. Macromolecules 2001, 34, 1864.
16. Koo, C. M.; Kim, J. H.; Wang, K. H.; Chung, I. J. J Polym Sci Part B: Polym Phys 2005, 43, 158.
17. Ramsay, J. D. F.; Lindner, P. J Chem Soc Faraday Trans 1993, 89, 4207.
18. Ramsay, J. D. F.; Swanton, S. W.; Bunce, J. J Chem Soc Faraday Trans 1990, 86, 3919.
19. Carreau, P. J.; De, K. D.; Chhabra, R. P. Rheology of Polymeric Systems Principles and Applications; Hanser Publisher: New York, 1997.
20. Ferry, J. D. Viscoelastic Properties of Polymers; John Wiley & Sons: New York, 1980.
21. Gu, S. Y.; Ren, J.; Wang, Q. F. J Appl Polym Sci 2004, 91, 2427.
22. Boyer, R. F.; Meier, D. J. Molecular Basis of Transitions and Relaxations; Gordon and Breach Science Publishers: New York, 1978; p 75.
23. McCrum, N. G.; Read, B. E.; Williams, G. An elastic and Dielectric Effects in Polymer Solids; John Wiley and Sons: London, 1967.